Received October 28, 2018, accepted November 15, 2018, date of publication November 19, 2018, date of current version December 18, 2018.

Digital Object Identifier 10.1109/ACCESS.2018.2882093

Dual-Layer Single-Varactor Driven Reflectarray Cell for Broad-Band Beam-Steering and Frequency Tunable Applications

SANDRA COSTANZO, (Senior Member, IEEE), FRANCESCA VENNERI, ANTONIO RAFFO, AND GIUSEPPE DI MASSA
Dipartimento di Ingegneria Informatica, Modellistica, Elettronica e Sistemistica, Università della Calabria, 87036 Rende, Italy
Corresponding author: Sandra Costanzo (costanzo@dimes.unical.it)

ABSTRACT A dual-layer active reflectarray configuration is proposed for broad-band beam-steering and/or frequency-tunable applications. A unit cell composed by two stacked fixed-size rectangular patches, properly loaded with a single varactor diode, is designed to realize the dynamic phase tuning mechanism. The proposed approach offers wider bandwidths, with respect to the existing varactor-based reflectarray cells, and quite good frequency reconfigurability features, as demanded by several radar or satellite communication applications. An X-band reflectarray cell is fabricated and tested, to prove the effectiveness of the proposed approach, achieving a 318° phase agility within a measured frequency range of about 14.6% with respect to the central design frequency (i.e., 11 GHz). Wideband beam-steering reflectarray designs are demonstrated, showing 1-dB gain bandwidths equal to 9–10%.

INDEX TERMS Reflectarray, varactor, beam-steering, wideband.

I. INTRODUCTION

Reconfigurable reflectarray antennas provide an appealing solution to meet the increasing demands of modern RF communication systems for reconfiguration capabilities, such as beam-steering, pattern re-shaping, multi-band operation, polarization flexibility or frequency agility. Several papers show the effectiveness of reflectarrays in satisfying one or more of the above tasks, through the use of tunable discrete components, such as pin/varactor diodes and Micro Electro-Mechanical Systems (MEMS), or electrically tunable materials, like liquid crystal (LC) or innovative graphene-based substrates [1]–[3]. The active reflectarrays presented in literature offer many advantages, such as low profiles, simpler architectures, instantaneous reconfiguration capabilities and increased efficiencies thanks to the use of spatial feeding. However, they are typically characterized by very narrow operating bandwidths that, in the case of reflectarrays with moderate aperture, are primarily limited by the frequency band of the single radiator [1]. As a consequence of this, the design of wideband reflectarray unit cells is the first task to be satisfied for obtaining wide bandwidth reflectarrays.

Many solutions have been developed to improve the bandwidth of passive reflectarray designs [1], [4]. They are usually based on the use of multi resonant elements, such as the ring-shaped radiating patch or the three-layer stacked cell, respectively proposed in [5] and [6]; the adoption of the aperture coupled configuration [7], or the use of closely spaced radiators [8]–[10]. Improved bandwidths ranging from 8% up to 19% are demonstrated in the above passive designs.

Currently, further efforts are needed in the development of wideband active reflectarray radiators, which are usually characterized by few percent bandwidths, as discussed in the following. A stub-tuned reflectarray cell loaded by two varactors is demonstrated in [11], which exhibits a 2.2% phase bandwidth, at 5.4 GHz, and a 3dB-gain bandwidth equal to 3.6 %. A 2.5% phase bandwidth is demonstrated in [12] at 5.4 GHz, for a single layer element, based on the use of a double square ring loaded with three pairs of varactor diodes. A beam switching reflectarray monolithically integrated with RF-MEMS switches is tested at 26.5GHz, showing a 3.77% bandwidth [13]. A 10 GHz-rectangular patch, aperture coupled to a pair of radial stubs loaded by a single varactor diode, is proposed by the authors in [14], showing a 3% phase bandwidth and a 6% 1dB-gain bandwidth (BW_{1dB}). A 35GHz unit cell, composed by three parallel microstrip dipoles placed over a tunable LC-substrate, is proposed in [15], achieving an extended 7%-bandwidth with respect to the existing LC-based reflectarrays.

In order to improve the bandwidth of varactor-based reflectarray configurations, a novel reconfigurable reflectarray cell, preliminarily introduced by Costanzo *et al.* [16], is proposed in this paper. It consists of two stacked fixed size rectangular patches tuned by a single varactor diode. In particular, a resonating patch, printed on the upper side of the stratified structure, is parasitically coupled to a varactor loaded patch beneath it. The stacked elements are properly designed to achieve a full phase tuning in the reflection coefficient of the unit cell.

The use of a stacked structure is a well-known technique to improve the instantaneous bandwidth of passive reflectarrays, due to the increased radiator-ground plane spacing and the multi resonant behavior [1], [10], [17]. The configuration proposed in this paper is the first example of varactor-based reconfigurable reflectarray, employing the patches-stacking concept as a bandwidth broadening approach. Furthermore, the proposed phase tuning mechanism allows to combine unit cell beam-scanning and/or reshaping pattern capabilities with frequency reconfigurability features, namely it is able to dynamically tune the reflection phase at variable frequencies, within a quite large frequency range. Unlike other configurations offering higher degree of frequency agility [18], the proposed reflectarray cell allows to achieve wider instantaneous bandwidths, by integrating a single DC-tunable lumped component (i.e. one varactor diode), thus preserving the relative simplicity of the biasing network.

In order to prove the effectiveness of the proposed configuration, a $0.55\lambda \times 0.55\lambda$ reflectarray cell is designed and tested to operate at a central frequency $f_0 = 11$GHz; in particular, a 318° phase agility is demonstrated within a 1.6GHz span (2 times greater than that achieved in [14]), corresponding to a 14.6% frequency range with respect to f_0. Furthermore, a quite wide instantaneous-bandwidth is achieved on a 65-elements reflectarray prototype, for different configurations of varactor diodes capacitances, giving a beam steering from 0° up to ±40°. As a matter of the fact, 9-10% 1-dB gain bandwidths are demonstrated from measured data, greater than those achieved in previous varactor-based designs [11]–[14].

The paper is organized as follows. Section II describes the geometry and the general design details of the proposed active reflectarray element, which is experimentally validated in Section III. Section IV shows the wideband behavior of the fabricated reflectarray prototype, in correspondences of some synthesized beam-steered radiation patterns. Conclusions are finally outlined in Section V, where some possible future developments are given for designing dual-band and/or dual-polarization varactor loaded reflectarray configurations.

II. REFLECTARRAY UNIT CELL GEOMETRY AND DESIGN

The active unit cell proposed in this work is illustrated in Fig.1. Two rectangular fixed size patches (i.e. the lower patch $L_1 \times W_1$ and the upper patch $L_2 \times W_2$ in Fig. 1(b)) are printed on two different stacked substrate layers, properly spaced each other with an air gap having a thickness, h_{air},

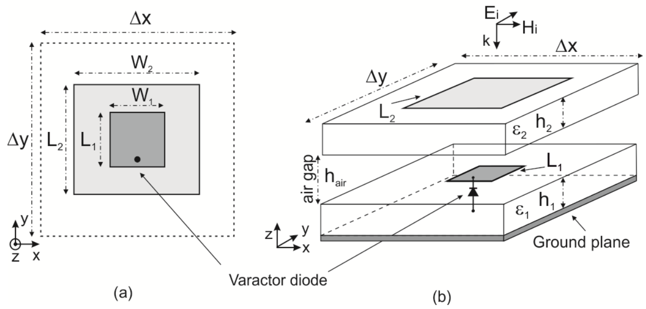

FIGURE 1. Unit cell geometry: (a) top view; (b) tridimensional view.

which assures an adequate parasitic coupling between the two patches (Fig. 1(a)). As depicted in Fig. 1, the lower patch is loaded by a shunt varactor diode, placed on one of its radiating edges, thus acting as a phase shifter able to realize the continuous phase tuning of the field reflected by the unit cell, when an impinging plane wave is considered (Fig. 1(a)). As a matter of the fact, the electrical length (i.e. the resonant frequency) of the lower patch is modified by the diode variable capacitive reactance [19], thus allowing a dynamic phase control of unit cell response.

Both patches are properly dimensioned to achieve a full phase tuning range at the desired frequency, by varying the diode capacitance within the values-range offered by the adopted varactor model. As compared to the single layer varactor-based cell proposed in [20], where the element bandwidth does not exceed 0.6%, the present configuration gives much broader instantaneous bandwidths, as demonstrated in the following Sections. As a matter of the fact, the use of a stacked structure allows to improve the antenna bandwidth [1], [17], due to the multi-resonant behavior and the increased radiator-ground plane spacing (i.e. $h_{tot} = h_2 + h_{air} + h_1$ in Fig. 1(a)), that in the case of the single layer varactor-loaded patch is fixed by the diode package height (i.e. h_1 in Fig. 1(a)) [20].

In order to prove the validity of the proposed active unit cell, a preliminary design is performed in this work within the X-band. The unit cell analysis is performed by adopting the infinite array approach and assuming a normally incident plane wave, with a y-oriented electric field component (Fig.1). The variable capacitive load in Fig. 1 is modeled with the equivalent circuit reported in [21] and [22], which considers the parasitic effects due to diode package, consisting of a 0.15pF parallel capacitance and a 0.2nH series inductance. The unit cell is designed to give a quite full phase tuning range at 11 GHz, by varying the diode capacitance C_{var} from 0.2 pF up to 2 pF. The package of the adopted varactor diode has cylindrical shape, with a radius and height respectively equal to 1.27 mm and 0.762 mm [23]. The synthesized $0.55\lambda \times 0.55\lambda$-cell (Fig. 1) consists of: a lower patch, $L_1 \times W_1 = 5.4\text{mm} \times 5.3\text{mm}$, printed on a grounded dielectric slab having a dielectric constant $\varepsilon_r = 2.33$ (i.e. Diclad870) and the same height of the adopted varactor model (i.e. $h_1 = 0.762$mm); an upper patch, $L_2 \times W_2 =$

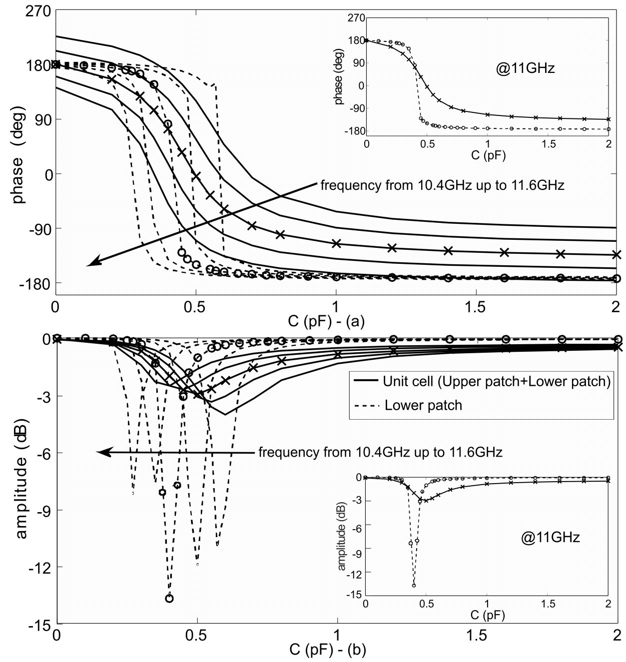

FIGURE 2. Simulated reflection coefficient vs. diode capacitance for different frequencies: (a) phase; (b) amplitude.

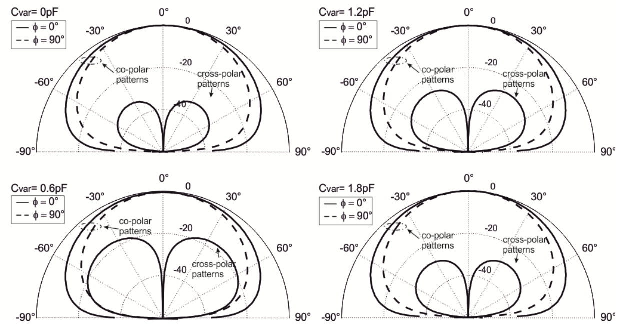

FIGURE 3. Simulated co-polar and cross-polar patterns of the proposed unit cell for different diode capacitance values C_{var}

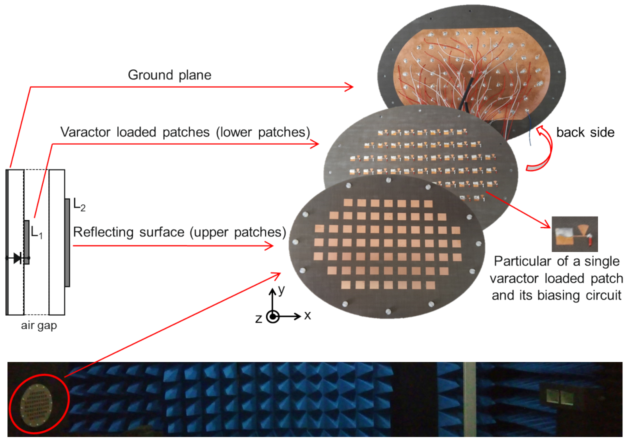

FIGURE 4. Reflectarray prototype layers and reflection phase measurement setup.

8.3mm × 9.5*mm*, printed on a substrate composed by a 0.762-mm-thick layer of Diclad870 and a layer of air having a thickness h_{air} = 0.762mm. The above dimensions are chosen in accordance with the following design rules.

Firstly, the varactor loaded patch (i.e. the lower patch $L_1 \times W_1$ in Fig. 1), is properly sized to achieve a full phase tuning range at the operating frequency f_0 (see Fig. 2(a)), without considering the upper patch (Fig. 1(a)).

Afterwards, an additional passive resonating patch (i.e. the upper patch $L_2 \times W_2$) is placed above the varactor loaded patch (Fig. 1(a)), in order to enhance the unit cell operating bandwidth [17] while preserving, at the same time, the effectiveness of the previously implemented phase tuning mechanism (Fig. 2(a)).

The simulated results, depicted in Fig. 2(a), show that by changing the diode capacitance C_{var} from 0.2 pF up to 2 pF, the proposed unit cell offers a phase variation range of about 315° in a neighborhood of the design frequency f_0 = 11 GHz.

Smoother phase variation can be observed with respect to the single layer case, depicted in the same figure, thus demonstrating a wider bandwidth behavior. Furthermore, as illustrated in Fig. 2(b), the use of a stacked configuration allows to reduce the unit cell losses, due to the increased total thickness h_{tot} of the assumed substrates stratification [24].

As a matter of the fact, the maximum losses provided by the proposed stacked configuration are about equal to −3 dB, at the operating frequency f_0 = 11 GHz (see the details box in Fig. 2(b)), against the −13 dB losses given by the single layer structure. In addition, the proposed unit cell shows reasonably low cross-polar components, that in the worst case (i.e. C_{var} = 0.6 pF) are 20dB smaller with respect to the co-polar patterns, as illustrated in Fig. 3, where both the co-polar as well as the cross-polar patterns are computed for different varactor capacitance values (i.e. C_{var} = 0, 0.6, 1.2 and 1.8 pF).

III. EXPERIMENTAL VALIDATION OF THE REFLECTARRAY CELL

In order to validate the proposed active configuration, the above designed unit cell is realized and tested in the Microwave Laboratory of the University of Calabria (Fig. 4). A far-field measurement setup [21], consisting of a couple of transmitting/receiving horn antennas, is adopted to detect the reflection phase of an array composed by 65 cells (Fig. 4), loaded by identically biased varactors (Microsemi MV31011-89 [23]). A DC-biasing line is properly designed for each cell and printed on the layer hosting the varactor loaded patches (Fig. 4). It consists of a high impedance microstrip-line (i.e. Z_0 = 138Ω) parallel connected to a radial stub (Fig. 5(a)), that behaves as a RF-chock in a neighborhood of f_0 (Fig. 5(b)).

By changing V_{bias} from 0 V to 20 V, giving a diode junction capacity variation in the range from 2 down to 0.2 pF [23], a continuous phase shift up to 318° is obtained within the frequency range [10.4 ÷ 11.98] GHz, corresponding to an operational frequency band equal to 14.6% (Fig. 6(a)).

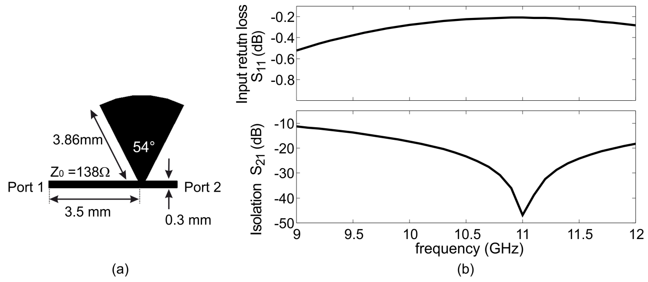

FIGURE 5. Biasing line design: (a) layout of the printed biasing line; (b) simulated scattering parameters.

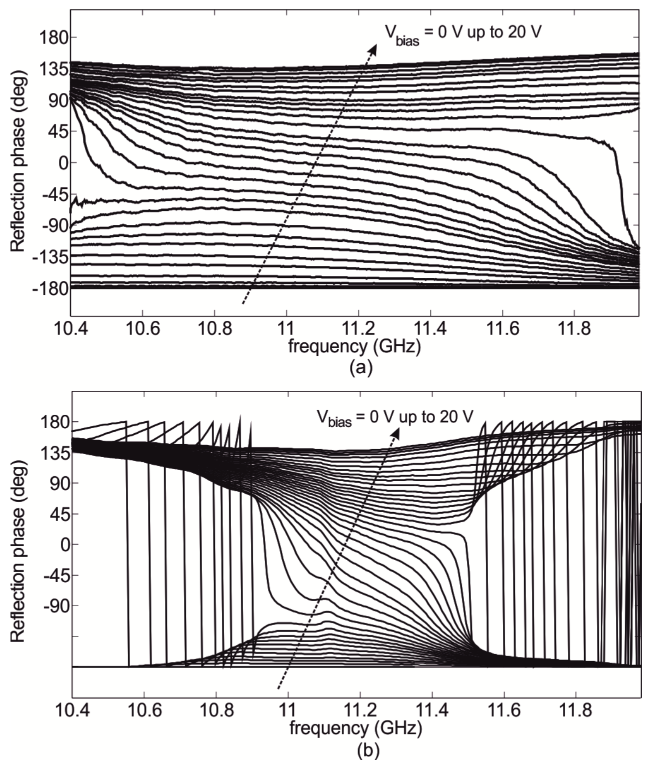

FIGURE 6. Measured reflection phase vs. frequency for different diode bias voltages: (a) proposed varactor loaded dual layer cell; (b) varactor loaded aperture coupled cell (linear phasing line) [21].

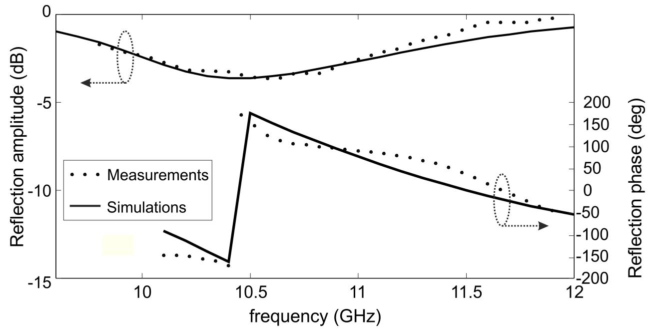

FIGURE 7. Comparison between measured and simulated reflection coefficient vs. frequency for $V_{bias} = 8V$.

TABLE 1. Frequency agility of different varactor-based cells.

Cell Configuration	Operating frequency band (Measurements) Lower Frequency (GHz)	Upper Frequency (GHz)	%
Dual-layer patch [present work]	10.4	11.98	14.5
Aperture-coupled patch [14] (varactor loaded radial line)	9.6	10.45	8.5
Aperture-coupled patch [21] (varactor loaded linear line)	11	11.5	4.4

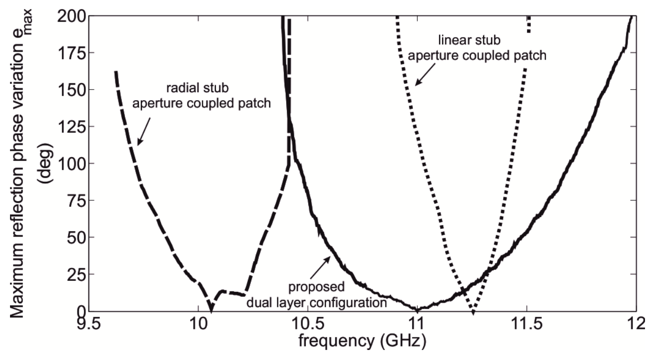

FIGURE 8. Maximum reflection phase variation e_{max} (f) evaluated on the measured phase curves *vs.* frequency for different V_{bias}-values: comparison between the proposed cell and the aperture coupled cells proposed by authors in [14] and [21].

An improved reconfiguration frequency range, increasing from 4.4% up to 14.6% (see Fig. 6(a)-(b) and Table 1), can be observed with respect to the varactor-loaded aperture coupled cells, proposed by the same authors in [14] and [21].

As depicted in Fig. 7, illustrating the reflection coefficient of the proposed cell evaluated for a V_{bias} value equal to 8V, a very good agreement is achieved between simulations and measurements.

Furthermore, the measured phase curves, illustrated in Fig. 6(a), are almost parallel within the considered frequency range, thus revealing a wideband behavior. As a matter of the fact, by adopting the standardized bandwidth definition on the reflection phase curves [11], it is possible to observe a wider band behavior in a neighborhood of the central design frequency with respect to the existing varactor-based reflectarray configurations.

Defining the maximum reflection phase variation as [11], [14]:

$$e_{max}(f) = \max_{V_{bias}} |\psi(f) - \psi(f_0)| - \min_{V_{bias}} |\psi(f) - \psi(f_0)| \quad (1)$$

and assuming the unit cell instantaneous bandwidth as the frequency range within which $e_{max}(f) \leq 22.5°$ (see Fig. 8), a 660 MHz band (≅6% at 11 GHz) is achieved against: the 119 MHz-band (2.2% at 5.4 GHz) demonstrated in [11] for the stub-tuned reflectarray cell loaded by two varactors; the 130 MHz-band (2.5% at 5.4 GHz) achieved in [12], for the double square ring loaded with three pairs of varactor diodes; the 140 MHz (1.2% at 11.25 GHz) and the 300 MHz (3% at 10 GHz) bands, respectively measured by the authors in [21] and in [14], for the single varactor loaded aperture coupled configurations.

TABLE 2. Phase curve bandwidth of different varactor-based cells.

Cell Configuration	Frequency	Phase curve BW (1)
Dual-layer patch [present work]	11 GHz	6 %
Aperture-coupled patch [14] (varactor loaded radial line)	10 GHz	3 %
Aperture-coupled patch [21] (varactor loaded linear line)	11.25 GHz	1.2 %
Stub-tuned cell loaded by two varactors [11]	5.4 GHz	2.2 %
Double square ring loaded with three pairs of varactor diodes [12]	5.4 GHz	2.5 %
Single layer varactor loaded patch [20]	5 GHz	0.6 %

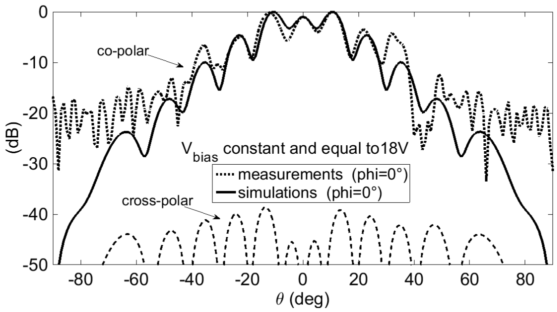

FIGURE 9. Normalized radiation pattern for a uniform varactors bias voltages distribution (H-plane).

These last configurations are compared in Fig. 8 with the dual-layer configuration proposed in this work, while a more exhaustive comparison with other structures is reported in Table 2.

IV. DESIGN OF BEAM-STEERING REFLECTARRAY ANTENNAS

The reconfigurability features of the designed reflectarray prototype are properly verified by changing the biasing voltages across the diodes, in order to realize the beam steering function. The varactor voltages distributions are computed by adopting a synthesis procedure that receives as input the desired radiation pattern, in terms of main beam direction and maximum side lobes level, and automatically returns the required excitation phase on each reflectarray element [21]. This last data are retrieved from the measured phase curves depicted in Fig. 6(a). The fabricated 65-elements prototype (Fig. 4), is illuminated by a X-band horn, which is placed in the E-plane (i.e. the yz-plane in Figs. 4, 10(b)), at a distance of 32.5 cm from the reflecting surface, with an offset angle of about 15°. To verify the beam-scanning operation mode, the synthesis algorithm is applied for obtaining the correct phase distributions giving a main beam pointed to some specific directions in the H-plane (i.e. the xz-plane in Figs. 4, 10(b)). As a starting point, the reflectarray behavior is considered in the absence of a proper phase distribution compensating for the phase delay imposed by the feed. The corresponding theoretical and experimental H-plane patterns, obtained at 11 GHz for a uniform voltage supply of 18 V on each varactor, are illustrated in Fig. 9.

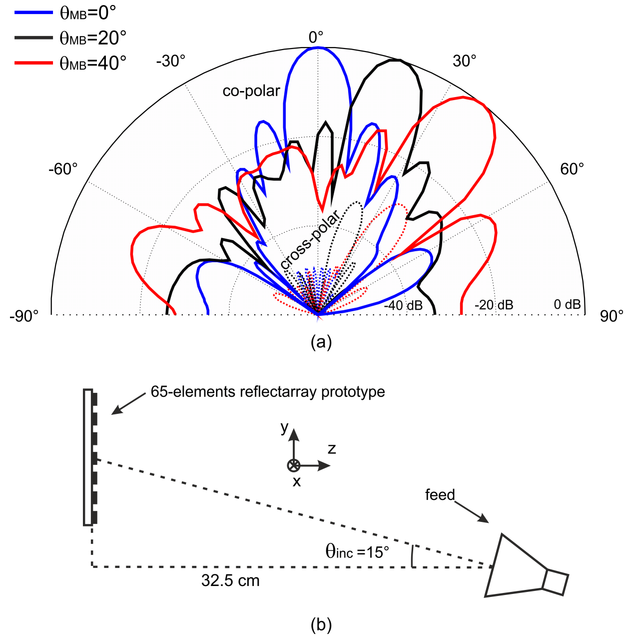

FIGURE 10. Normalized radiation patterns (H-plane) for different varactors bias voltage distributions (a) and a schematic layout of the designed reflectarray prototype.

Conversely, Fig. 10(a) shows the synthesized patterns (@11 GHz) obtained for some bias voltages distributions compensating for the phase delay imposed by the feed and giving at the same time the main-lobe steered towards the directions $\theta_{MB} = 0°, 20°$, and $40°$, in the H-plane. Low cross-polar components, smaller than -30dB, can be observed in Figs. 9 and 10(a).

In order to better appreciate the wider band behavior of the proposed active phase scanning mechanism, the instantaneous bandwidth of the fabricated reflectarray prototype is also evaluated in terms of 1dB gain-bandwidth (i.e. BW_{1dB}), for each synthesized beam steered radiation pattern (Fig. 10). This analysis allows to demonstrate the broad-band beam-steering capabilities offered by the proposed approach, with respect to the existing active reflectarray configurations [11]–[14] and the usually adopted phase-shifters [25]. As a matter of the fact, the array theory states that the more severe bandwidth limitation in beam-scanned arrays is caused by the use of phase shifters instead of time-delay devices [25], as they usually allow to scan the beam along the desired angle only at the central frequency f_0. The following formula, giving the half power fractional bandwidth of a beam-scanned array having a length L and driven by single frequency phase shifters, clearly shows that the array bandwidth becomes smaller as the array is made larger or as the scan angle θ_0 is increased [25]:

$$\frac{\Delta f}{f_0} \approx 0.886 \left(\frac{\lambda}{L \sin \theta_0} \right) \tag{2}$$

Thus, a phase tuning mechanism able to introduce the desired phase shift within a wider frequency band is the first task to be satisfied to realize a broad-band beam-steering.

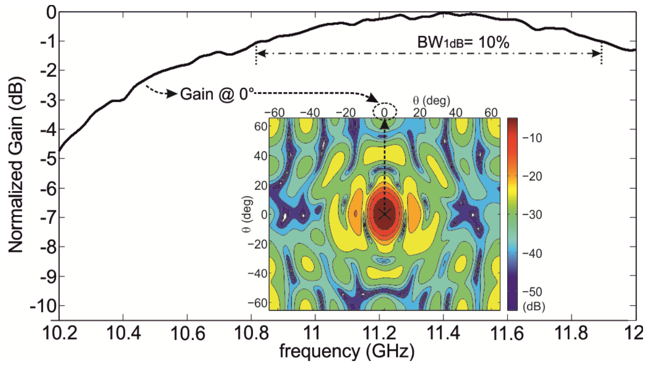

FIGURE 11. Gain pattern vs. frequency at $\theta = 0°$ in the H-plane and the corresponding synthesized E-field contour plot (normalized values).

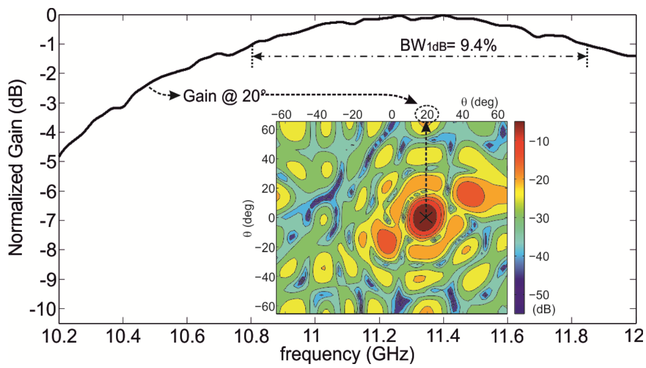

FIGURE 12. Gain pattern vs. frequency at $\theta = 20°$ in the H-plane and the corresponding synthesized E-field contour plot (normalized values).

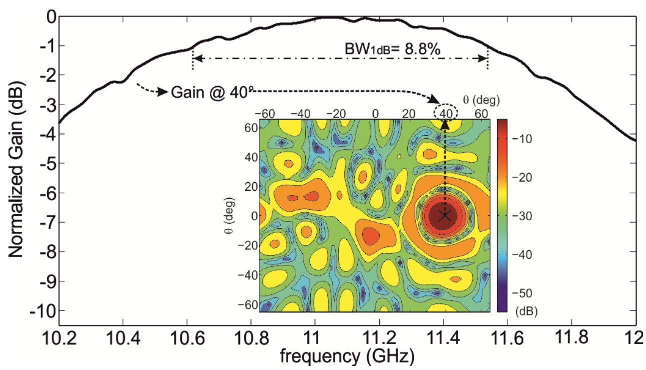

FIGURE 13. Gain pattern vs. frequency at $\theta = 40°$ in the H-plane and the corresponding synthesized E-field contour plot (normalized values).

In the case of the proposed configuration, the gain patterns versus frequency (Figs. 9-11), evaluated along the synthesized main beam directions of Fig. 8(a), show good and quite similar BW_{1dB} values equal to: 10%, for $\theta_{MB} = 0°$, 9.4%, for $\theta_{MB} = 20°$ and 8.8%, for $\theta_{MB} = 40°$.

The above values give wider bandwidth as compared to those achieved in previous works [11], [14]. As a matter of the fact, a value $BW_{3dB} = 200$ MHz (3.6%) is demonstrated in [11] at 5.4 GHz, while a BW_{1dB} of about 6% is achieved by Costanzo *et al.* [14], for a 15° -steered H-plane pattern. Furthermore, a low impact of the scan angle variations on the reflectarray BW_{1dB} can be observed in Figs. 11-13. As a matter of the fact, a BW_{1dB} reduction of just 7% can be observed in the 40° -scanned pattern (Fig. 13) with respect to the 20° -scanned pattern (Fig. 12).

Conversely, equation (2) states that an array of the same length (i.e. L = 16.5cm along the scanning plane, namely the H-plane), driven by single frequency phase shifters, shows a bandwidth reduction that is inversely proportional to the $\sin\theta_0$ function, thus giving a 46% bandwidth variation between the 40° and the 20° -scanned patterns.

Furthermore, a maximum gain of about 16.6 dB ($\theta_{MB} = 0°$), 16.3 dB ($\theta_{MB} = 20°$) and 15.4 dB ($\theta_{MB} = 40°$) is achieved, corresponding to an aperture efficiency respectively equal to 18.3%, 17.2%, 14%. These quite low efficiency values are essentially due to the small size of the reflecting surface, which causes high spillover losses. Anyhow, the reflectarray prototype is designed with the only purpose of verifying the broadband skills of the proposed tunable configuration; therefore, the other antenna performances are not optimized.

In conclusion, the above results confirm the wider band behavior of the proposed active phase tuning mechanism in realizing the beam steering function, with respect to the existing varactor-based reflectarray configurations [11]–[14].

V. CONCLUSIONS

A novel active reflectarray configuration has been proposed in this paper for broad-band beam-steering applications. The adopted element, based on the use of a couple of stacked rectangular patches, loaded with a single varactor diode, has been optimized for a full phase tuning range. Simulated and measured data have been reported to demonstrate the phase tuning ability of the proposed configuration, showing good reconfiguration capabilities within a quite large frequency band equal to 14.6%, within the X-band. A wider bandwidth behavior, with respect to the existing varactor-based reflectarray cells, has been demonstrated in terms of measured phase curves. Wideband beam-steering designs have been demonstrated on a 65-elements reflectarray, showing 1-dB gain bandwidths about equal to 9-10%, for different scan angles. In conclusion, the proposed approach offers wider bandwidths, with respect to the existing varactor-based reflectarray cells, and quite good frequency reconfigurability features, as demanded by several RF applications.

Due to the current trend toward dual-band/dual-polarization applications [2], [26], [27], the proposed broadband varactor loaded configuration will be further investigated to incorporate the above skills. Both the patches stacking concept as well as the antennas miniaturization solutions, proposed by the authors in [28], [29], will be adopted to integrate in the same unit cell more patches working in a dual band/dual polarization operation mode.

REFERENCES

[1] J. Huang and J. Encinar, *Reflectarray Antennas*. Hoboken, NJ, USA: Wiley, 2008.

[2] S. V. Hum and J. Perruisseau-Carrier, "Reconfigurable reflectarrays and array lenses for dynamic antenna beam control: A review," *IEEE Trans. Antennas Propag.*, vol. 62, no. 1, pp. 183–198, Jan. 2014.
[3] P. Nayeri, F. Yang, and A. Z. Elsherbeni, "Beam-scanning reflectarray antennas: A technical overview and state of the art," *IEEE Antennas Propag. Mag.*, vol. 57, no. 4, pp. 32–47, Aug. 2015.
[4] M. H. Dahri, M. H. Jamaluddin, M. Inam, and M. R. Kamarudin, "A review of wideband reflectarray antennas for 5G communication systems," *IEEE Access*, vol. 5, pp. 17803–17815, Aug. 2017.
[5] M. R. Chaharmir, J. Shaker, N. Gagnon, and D. Lee, "Design of broadband, single layer dual-band large reflectarray using multi open loop elements," *IEEE Trans. Antennas Propag.*, vol. 58, no. 9, pp. 2875–2883, Sep. 2010.
[6] J. A. Encinar and J. A. Zornoza, "Broadband design of three-layer printed reflectarrays," *IEEE Trans. Antennas Propag.*, vol. 51, no. 7, pp. 1662–1664, Jul. 2003.
[7] E. Carrasco, M. Barba, and J. A. Encinar, "Reflectarray element based on aperture-coupled patches with slots and lines of variable length," *IEEE Trans. Antennas Propag.*, vol. 55, no. 3, pp. 820–825, Mar. 2007.
[8] D. M. Pozar, "Wideband reflectarrays using artificial impedance surfaces," *Electron. Lett.*, vol. 43, no. 3, pp. 148–149, Feb. 2007.
[9] F. Venneri, S. Costanzo, and G. Di Massa, "Bandwidth behavior of closely spaced aperture-coupled reflectarrays," *Int. J. Antennas Propag.*, vol. 2012, Jun. 2012, Art. no. 846017, doi: 10.1155/2012/846017.
[10] P. Nayeri, F. Yang, and A. Z. Elsherbeni, "Broadband reflectarray antennas using double-layer subwavelength patch elements," *IEEE Antennas Wireless Propag. Lett.*, vol. 9, pp. 1139–1142, 2010.
[11] M. Riel and J. J. Laurin, "Design of an electronically beam scanning reflectarray using aperture-coupled elements," *IEEE Trans. Antennas Propag.*, vol. 55, no. 5, pp. 1260–1266, May 2007.
[12] C. Liu and S. V. Hum, "An electronically tunable single-layer reflectarray antenna element with improved bandwidth," *IEEE Antennas Wireless Propag. Lett.*, vol. 9, pp. 1241–1244, 2010.
[13] O. Bayraktar, O. A. Civi, and T. Akin, "Beam switching reflectarray monolithically integrated with RF MEMS switches," *IEEE Trans. Antennas Propag.*, vol. 60, no. 2, pp. 854–862, Feb. 2012.
[14] S. Costanzo, F. Venneri, A. Raffo, G. Di Massa, and P. Corsonello, "Radial-shaped single varactor-tuned phasing line for active reflectarrays," *IEEE Trans. Antennas Propag.*, vol. 64, no. 7, pp. 3254–3259, Jul. 2016.
[15] G. Perez-Palomino, J. A. Encinar, M. Barba, and E. Carrasco, "Design and evaluation of multi-resonant unit cells based on liquid crystals for reconfigurable reflectarrays," *IEE Microw. Antennas Propag.*, vol. 6, no. 3, pp. 348–354, Feb. 2012.
[16] S. Costanzo, F. Venneri, G. Di Massa, A. Borgia, and A. Raffo, "Bandwidth performances of reconfigurable reflectarrays: state of art and future challenges," *Radioengineering*, vol. 27, no. 1, pp. 1–9, 2018.
[17] J. A. Encinar, "Design of two-layer printed reflectarrays using patches of variable size," *IEEE Trans. Antennas Propag.*, vol. 49, no. 10, pp. 1403–1410, Oct. 2001.
[18] D. Rodrigo, L. Jofre, and J. Perruisseau-Carrier, "Unit cell for frequency-tunable beamscanning reflectarrays," *IEEE Trans. Antennas Propag.*, vol. 61, no. 12, pp. 5992–5999, Dec. 2013.
[19] P. Barthia and J. Bahl, "Frequency agile microstrip antennas," *Microw. J.*, vol. 25, pp. 67–70, Oct. 1982.
[20] L. Boccia, G. Amendola, and G. Di Massa, "Performance improvement for a varactor-loaded reflectarray element," *IEEE Trans. Antennas Propag.*, vol. 58, no. 2, pp. 585–589, Feb. 2010.
[21] F. Venneri, S. Costanzo, and G. Di Massa, "Design and validation of a reconfigurable single varactor-tuned reflectarray," *IEEE Trans. Antennas Propag.*, vol. 61, no. 2, pp. 635–645, Feb. 2013.
[22] F. Venneri, S. Costanzo, and G. Di Massa, "Tunable reflectarray cell for wide angle beam-steering radar applications," *J. Electr. Comput. Eng.*, vol. 2013, Jul. 2013, Art. no. 325746, doi: 10.1155/2013/325746.
[23] *Microsemi Design Support*. [Online]. Available: http://www.microsemi.com/en/design-support/
[24] F. Costa and A. Monorchio, "Closed-form analysis of reflection losses in microstrip reflectarray antennas," *IEEE Trans. Antennas Propag.*, vol. 60, no. 10, pp. 4650–4660, Oct. 2012.
[25] R. J. Mailloux, *Phased Array Antenna Handbook*, 2nd ed. Norwood, MA, USA: Artech House, 2005.
[26] J. Perruisseau-Carrier, "Dual-polarized and polarization-flexible reflective cells with dynamic phase control," *IEEE Trans. Antennas Propag.*, vol. 58, no. 5, pp. 1494–1502, May 2010.
[27] C. Guclu, J. Perruisseau-Carrier, and O. Civi, "Proof of concept of a dual-band circularly-polarized RF MEMS beam-switching reflectarray," *IEEE Trans. Antennas Propag.*, vol. 60, no. 11, pp. 5451–5455, Nov. 2012.
[28] S. Costanzo and F. Venneri, "Miniaturized fractal reflectarray element using fixed-size patch," *IEEE Antennas Wireless Propag. Lett.*, vol. 13, pp. 1437–1440, Jul. 2014.
[29] S. Costanzo, F. Venneri, G. Di Massa, A. Borgia, A. Costanzo, and A. Raffo, "Fractal reflectarray antennas: State of art and new opportunities," *Int. J. Antennas Propag.*, vol. 2016, Sep. 2016, Art. no. 7165143, doi: 10.1155/2016/7165143.

SANDRA COSTANZO (SM'12) received the Laurea degree *(summa cum laude)* in computer engineering from the University of Calabria, Italy, in 1996, and the Ph.D. degree in electronic engineering from the University of Reggio Calabria in 2000. She is currently an Associate Professor at the University of Calabria, where she teaches the courses of electromagnetic waves propagation, remote sensing and radar systems, and electromagnetic diagnostics. At the University of Calabria, she is also the Coordinator of the master degree course in telecommunication engineering. Since 1996, she has been involved in many research projects funded by the European Space Agency, the Agenzia Spaziale Italiana, Ministero dell'Istruzione, dell'Università e della Ricerca, and private companies. She has been an editor of two books and a lead editor of three special issues on international journals. She has (co-)authored over 170 contributions in international journals, books, and conferences. Her research interests are focused on near-field far-field techniques, antenna measurement techniques, antenna analysis and synthesis, numerical methods in electromagnetics, millimeter-wave antennas, reflectarrays, microwave sensors for biomedical applications, microwave imaging, electromagnetic characterization of materials, innovative antennas, and technologies for radar applications. She is a member of the IEEE South Italy Geoscience and Remote Sensing Chapter, the CNIT (Consorzio Nazionale Interuniversitario per le Telecomunicazioni), and the SIEm (Società Italiana di Elettromagnetismo), and a Board Member of the IEEEAP/ED/MTT North Italy Chapter and the IEEE Information Theory Italy Chapter. She is an Associate Editor of the IEEE ANTENNAS AND WIRELESS PROPAGATION LETTERS, the IEEE ACCESS, and the IEEE JOURNAL OF ELECTROMAGNETICS, RF AND MICROWAVES IN MEDICINE AND BIOLOGY, and a member of the Editorial Board of *Radioengineering* and the *International Journal of RF and Microwave Computer-Aided Engineering*.

FRANCESCA VENNERI received the degree in information technology engineering from the University of Calabria, Italy, in 1998, and the Ph.D. degree in electronic engineering from the Mediterranea University of Reggio Calabria in 2002. She is currently an Assistant Professor at the University of Calabria. Her research interests focus on microstrip reflectarrays, antenna analysis and synthesis, RFID technology, and metamaterial absorbers. She is a member of the IEEE Antennas and Propagation Society, the SIEm (Società Italiana di Elettromagnetismo), and the CNIT (Consorzio Consorzio Nazionale Interuniversitario per le Telecomunicazioni).

ANTONIO RAFFO received the master's degree in electronic engineering and the Ph.D. degree in ICT from the University of Calabria in 2012 and 2018, respectively. From 2012 to 2014, he was with the Department of Informatics, Modeling, Electronic and System Engineering within a National Italian Project on radar techniques for landslides risk mitigation. His research interests are focused on electromagnetic techniques for physiological sensing, electromagnetic characterization of materials, software-defined radio applications, and reconfigurable RF solutions. He has co-authored various contributions in national and international journal and conferences.

GIUSEPPE DI MASSA was born in Barano d'Ischia, Naples, Italy, in 1948. He received the Laurea degree in electronic engineering from the University of Naples Federico II, Naples, in 1973.

From 1978 to 1979, he was a Professor of antennas at the University of Naples, Italy. In 1980, he joined the University of Calabria, Italy, as a Professor of electromagnetic waves. He has been with the University of Calabria as an Associate Professor since 1985 and as a Full Professor since 1994, where he teaches antennas and electromagnetic fields. From 1985 to 1986, he was a Scientific Associate at CERN, Geneva. In 1988, he was a Visiting Professor at the Brookhaven National Laboratory, Long Island, NY, USA. From 1997 to 2002, he was the Dean of the Department of Elettronica, Informatica and Sistemistica and the President of the Programming Committee, University of Calabria. From 2000 to 2017, he was the Chairman of the Telecommunication Engineering Program, University of Calabria. He was the Italian Delegate in the European COST 284 Innovative Antennas for Emerging Terrestrial and Space-Based Applications from 2002 to 2006 and in the COST Action IC0603: Antenna Systems & Sensors for Information Society Technologies from 2007 to 2011. From 2011 to 2014, he was the Italian Delegate in the Management Committee of the COST Action IC1102, Versatile Integrated and Signal-aware Technologies for Antennas. From 2003 to 2007, he participated in the Network of Excellence Antenna Centre of Excellence, where he was a part of the Governing Board and a Leader of the Work Group WP 1.2-1: Antenna Measurement Services.

He has authored/co-authored over 300 scientific papers, mainly on international scientific journals or proceedings of international conferences. He is a principal investigator or coordinator of many research programs, granted by national and international research organizations and by leading national companies. His main research interests are focused on applied computational electromagnetics, microstrip antennas, microwave integrated circuits, reflectarrays, Gaussian beam solutions, millimeter-wave antennas, near-field measurements, electromagnetic characterization of materials, and innovative radar antennas and technologies.